Cerebral Cortex, 2019;00: 1–15

doi: 10.1093/cercor/bhz083
Advance Access Publication Date: 29 April 2019
Original Article

Downloaded from https://academic.oup.com/cercor/advance-article-abstract/doi/10.1093/cercor/bhz083/5480315 by Tufts University user on 29 April 2019

ORIGINAL ARTICLE

Synaptic Connectivity and Cortical Maturation Are Promoted by the ω-3 Fatty Acid Docosahexaenoic Acid

Beatrice E. Carbone[1,‡], Malik Abouleish[1,‡], Katherine E. Watters[1], Seth Vogel[1], Adema Ribic[1], Olaf H.-U. Schroeder[2], Benjamin M. Bader[2] and Thomas Biederer[1,†]

[1]Department of Neuroscience, Tufts University School of Medicine, Boston, MA 02111, USA and [2]NeuroProof GmbH, Friedrich Barnewitz-Str. 4, 18119 Rostock, Germany

Address correspondence to Thomas Biederer, 136 Harrison Avenue, Boston, MA 02111, USA. Email: thomas.biederer@tufts.edu; Tel.: +1 (617) 636-2131; Fax: +1 (617) 636-2413.

[‡]Shared first authors
[†]Thomas Biederer, http://orcid.org/0000-0003-0912-1514

Abstract

Brain development is likely impacted by micronutrients. This is supported by the effects of the ω-3 fatty acid docosahexaenoic acid (DHA) during early neuronal differentiation, when it increases neurite growth. Aiming to delineate DHA roles in postnatal stages, we selected the visual cortex due to its stereotypic maturation. Immunohistochemistry showed that young mice that received dietary DHA from birth exhibited more abundant presynaptic and postsynaptic specializations. DHA also increased density and size of synapses in a dose-dependent manner in cultured neurons. In addition, dendritic arbors of neurons treated with DHA were more complex. In agreement with improved connectivity, DHA enhanced physiological parameters of network maturation in vitro, including bursting strength and oscillatory behavior. Aiming to analyze functional maturation of the cortex, we performed in vivo electrophysiological recordings from awake mice to measure responses to patterned visual inputs. Dietary DHA robustly promoted the developmental increase in visual acuity, without altering light sensitivity. The visual acuity of DHA-supplemented animals continued to improve even after their cortex had matured and DHA abolished the acuity plateau. Our findings show that the ω-3 fatty acid DHA promotes synaptic connectivity and cortical processing. These results provide evidence that micronutrients can support the maturation of neuronal networks.

Key words: docosahexaenoic acid, synapse, visual acuity, visual cortex

Introduction

Synapse formation is instructed by genetic programs that control synapse-organizing mechanisms, and neuronal connectivity is refined by activity-dependent processes (Goda and Davis 2003; Shen and Scheiffele 2010; Benson and Huntley 2012; Schreiner et al. 2017). Parallel roles of dietary factors in shaping neuronal connectivity, specifically how micronutrients affect the synaptic wiring of developing neurons, are much less understood.

Gaining insights into the optimal intake of dietary micronutrients may be particularly relevant for infant health due to the prolonged time course of brain development in humans. A broad number of micronutrients are provided to infants by

© The Author(s) 2019. Published by Oxford University Press. All rights reserved. For permissions, please e-mail: journals.permissions@oup.com

breastfeeding. Among the micronutrients present in breast milk is the ω-3 fatty acid docosahexaenoic acid (DHA) that likely is essential in humans (Muskiet et al. 2004). It is more abundant in the cerebral cortex of breast-fed infants than in infants fed with formula lacking DHA (Makrides et al. 1994). Clinical studies have shown that breastfeeding improves children's cognitive development (Lucas et al. 1992; Anderson et al. 1999; McCann and Ames 2005; Kramer et al. 2008). It has been proposed that the higher proportion of DHA in the brain of breast-fed infants may partially explain this beneficial effect of breastfeeding (Makrides et al. 1994).

DHA is highly enriched in the brain compared with other tissues and modulates critical steps of early neuronal differentiation, including neurogenesis and neurite growth (Bourre 2004; Marszalek and Lodish 2005; Innis 2008; Bazinet and Laye 2014), and cortical DHA has neurotrophic and protective effects (Högyes et al. 2003; Wu et al. 2004). On a subcellular level, this ω-3 fatty acid is a prominent component of synaptosomal plasma membranes (Breckenridge et al. 1972). Possible roles of DHA abundance in synapse development are indicated by the gradual accumulation of ω-3 unsaturated fatty acids at maturing forebrain synapses (Tulodziecka et al. 2016) at a rate that tracks the rapid increase in excitatory synapse number in postnatal cortical development (Rakic et al. 1986; Micheva and Beaulieu 1996), and they reach a share of almost 20% of synaptic phospholipids in the mature brain. In agreement with a functional relevance of DHA as synaptic lipid, it regulates the expression of synaptic proteins and excitatory transmission (Cao et al. 2009; Kim et al. 2011a; Sidhu et al. 2011; Igarashi et al. 2015; Lozada et al. 2017).

DHA supplementation has beneficial effects on cognition not only in children but also in adult humans (McCann and Ames 2005). In turn, DHA deficiency in humans is correlated with attention deficits and increased schizophrenia risk (McNamara and Carlson 2006). A relevance of DHA for cognitive functions is supported by memory impairments in DHA-restricted mice (Moriguchi et al. 2000), and mice lacking the DHA transporter Mfsd2a exhibit deficits in learning and memory (Nguyen et al. 2014). A systematic analysis of how this micronutrient impacts connectivity and brain function can hence provide important insights.

Aiming to define DHA effects on brain maturation, we chose to focus on the visual cortex as the visual system is well suited to study the postnatal development of neuronal connectivity (Katz and Shatz 1996). This revealed that DHA supplementation from birth increased synaptic abundance in the visual cortex of young mice. Studies of dissociated neurons showed that DHA treatment potently increased the assembly of presynaptic and postsynaptic specializations. These effects were accompanied by substantial improvements in the physiological maturation of network properties. Moreover, in vivo recordings demonstrated that dietary DHA profoundly enhanced the maturation of cortical input processing as demonstrated by increased visual acuity. These results provide evidence that this ω-3 fatty acid promotes the development of synaptic connectivity and cortical function.

Materials and Methods

DHA Preparation

DHA-rich Single Cell Oil (DHASCO) vegetable oil containing 40% DHA was provided by Mead Johnson Nutrition, Global Discovery and packaged in a low oxygen atmosphere. DHA was prepared and aliquoted under an atmosphere of N_2 to prevent oxidation and was diluted in dimethyl sulfoxide (DMSO) prior to treatment of cultured neurons for immunocytochemical analysis. 76 mM DHA stocks were prepared by dissolving 25 mg DHA in 1.0 ml DMSO, aliquots for single use were made, and aliquots were stored at –80°C. For microelectrode array experiments (MEAs) of cultured neurons, DHA was purchased from Sigma (Cat# D2534), diluted at 100 mM in DMSO (Fisher Cat# D12345), and stored at −80 °C at low oxygen atmosphere.

DHA Administration to Mice

Infant nutrition-grade DHASCO vegetable oil containing 40% DHA was provided by Mead Johnson Nutrition, Global Discovery and packaged in a low oxygen atmosphere. A 4-oil blend containing palm olein, coconut, soybean, and high oleic sunflower oils was used as vegetable oil vehicle and was provided by Mead Johnson Nutrition. Aliquots of DHA working solutions were prepared once a week at 300 mg DHA/g oil by diluting DHASCO oil into the vegetable oil blend under a N_2 atmosphere to prevent oxidation. DHA was administered at 300 mg DHA/kg bodyweight/day as in previous rodent studies (Gamoh et al. 1999; Sakamoto et al. 2007; Holguin et al. 2008), a dietary dose that increases DHA amount in cortex and hippocampus (Gamoh et al. 1999).

Mouse pups were obtained by breeding C57BL/6 mice from Charles River (Kingston, New York, USA). DHA or vegetable oil solutions were provided once daily to C57BL/6 mouse pups from the day after birth (defined as postnatal day 1; P1) until P28, P35, or P45, as described in the Results. Littermate mice were used for vehicle control data. Nutrients were delivered into the back of the oral cavity to trigger a swallowing reflex to ensure the complete delivery of the desired amount to the pups, delivering a volume of 1 µl DHA working solution/g body weight/day starting at P1 (Rice et al. 2007; Cimafranca et al. 2010). Mice between P1–P4 were held ventrally, and their abdomens were stroked to help with swallowing. Supplements were provided in addition to the milk animals received from the mother until weaning at P21. After weaning, supplements were delivered daily as above. Regular chow (Teklad Global 18% protein, Cat# 2918) was provided ad libitum.

In addition to orally administered DHA, pups received DHA from breast milk. The DHA amount in milk of mouse dams on a control diet is approximately 0.25% of the total fatty acid content, and this is stable 7–15 days postpartum (Oosting et al. 2015). C57Bl/6 mouse pups at P10 consume a mean amount of 0.95 ml milk/pup per 24 h (Rath and Thenen 1979), and the fat content of the breast milk pups receive at this stage is ∼11 mg/100 µl (Barnett and Dickson 1984). P10 mice therefore consume ∼105 mg fat/day, corresponding to ∼0.26 mg DHA, through breast milk intake. The additional oral delivery of DHA at P10, when the average weight of a pup is 5.0 g, was in the amount of 1.5 mg DHA/day, as 300 mg DHA/kg bodyweight/-day were administered. This amount of administered DHA is ∼6-fold higher than what pups receive from breast milk, and no pronounced drop in DHA intake is expected to occur after weaning.

Immunostaining, Microscopy, and Image Quantification of Brain Sections

Animals were transcardially perfused at P35 first with ice cold phosphate buffered saline (PBS) and then with 4% paraformalde-

Downloaded from https://academic.oup.com/cercor/advance-article-abstract/doi/10.1093/cercor/bhz083/5480315 by Tufts University user on 29 April 2019

hyde (PFA) in PBS, pH 7.4. Brains were isolated and postfixed overnight in 4% PFA and washed and stored in PBS (all at 4 °C). Brains were mounted in PBS and coronally sectioned at 60 µm using a vibrating microtome (Vibratome 1500, Harvard Apparatus, Holliston, MA). Sections were stored in PBS at 4 °C. For visual cortex analysis, slices were selected from the posterior cortex where the hippocampal formation had fully extended. Sections were first washed in PBS and blocked with 3% normal serum and 0.1% Triton-X 100 (Sigma) in PBS for 2 h at room temperature (RT). Primary antibodies were raised in rabbit against Homer 1 (Synaptic Systems Cat# 160003, RRID:AB_887730; 1:500) and in mouse against vGlut1 (UC Davis/NIH NeuroMab Facility Cat# 73-066, RRID:AB_10673111; 1:800). Secondary immunostaining was performed with anti-IgG1 Alexa 568 (Thermo Fisher Cat# A-21124, RRID:AB_2535766) or anti-rabbit Alexa 488 (Thermo Fisher Cat# A31566, RRID:AB_10374301) antibodies (all at 1:500). Antibodies were diluted in 3% normal serum and 0.1% Triton-X 100 in PBS and incubated for 48–72 h at 4 °C (primary antibodies) or overnight at 4 °C (secondary antibodies). Sections were probed either for Homer 1 or vGlut1. After incubation, sections were washed in PBS and floated on slides in distilled water before coverslipping with mounting medium (CFM-3, Citifluor, Hatfield, PA, USA). Confocal microscopy was performed on a Leica TCS SP8. Images were acquired with an ACS APO ×63 oil lens with 1.4 NA at 2048 × 2048 pixels. All images were acquired in binocular V1, layer IV, which was located by moving distally in a straight line originating from the crest of the dentate gyrus, according to mouse brain atlas (Paxinos and Franklin, 2004). Images were acquired blind to the condition.

Quantification of fluorescence intensities in these immunohistochemical stainings was performed with ImageJ. Optical sections of 3 µm thickness comprised of six 0.5 µm z-steps were imaged. In ImageJ, 2 adjacent z-steps were maximally projected to generate three 1.0 µm thick optical sections for analysis. To determine the background, fluorescence intensity of 4 smaller background regions of interest (ROIs) was measured, the average mean gray value was calculated, and this was multiplied by the area of the larger ROI in which Homer 1 or vGlut1 intensity was determined. This size-corrected background value was then subtracted from the sum of all pixel intensity values in the larger ROI to determine in ImageJ the corrected total region fluorescence as described (Burgess et al. 2010).

For quantification of synaptic puncta in immunostained sections, a modified machine–learning-based Intellicount algorithm was applied (Fantuzzo et al. 2017). Images were converted to 16 bit and channels analyzed separately. In the Intellicount interface, the background removal factor was set to 0, the default thresholds were applied, and analysis was performed on nested folders under the settings “single channel/greyscale” and “synapses”. Data were exported to GraphPad Prism 7 to be compiled.

60k per discussion
2019.06.21

Neuronal Culture Preparation and DHA Treatment

Cultures of hippocampal neurons for synaptic marker analyses were prepared at embryonic day E18 from Sprague Dawley rat pups (Charles River, Kingston, New York, USA) and plated at 45000 cells/ml onto 12 mm ∅ coverslips coated with poly-L-lysine, as described (Biederer and Scheiffele 2007). Neurons were cultured in 1 ml medium. Ara-C was added at 2 div to prevent glia overgrowth. Cultures were treated at 4 div with DHA or DMSO as vehicle control at the concentrations provided in the text, and again at 8 and 10 div with half a fresh dose by exchanging 0.5 ml of the medium with 0.5 ml of fresh nutrient-supplemented medium. Cultures were kept at 37 °C in a 5% CO_2 atmosphere.

For MEA experiments, time-pregnant NMRI mice were purchased from Charles River (Sulzfeld, Germany). Neuronal cultures for MEA studies were prepared from embryonic brain tissue harvested from E15 NMRI mice as previously described (Gramowski et al. 2006; Feng et al. 2018). Briefly, frontal cortex was dissociated enzymatically in DMEM10/10 (10% horse and 10% fetal calf serum) including papain and DNase I, cells were resuspended in DMEM10/10 containing 10 µg/ml laminin (Sigma) at a density of 7.5×10^6 cells/ml, and 150 000 cells were seeded onto each well of 48-well MEA neurochips (Axion Biosystems Inc., Atlanta, GA, USA). Each well contains an array of 16 embedded platinum electrodes resulting in a total of 768 channels. Prior to plating, MEAs were coated with freshly prepared 0.1% polyethyleneimine (Sigma Cat# 181978) dissolved in Borate buffer (Fisher Scientific Cat# 28341). Cultures were kept at 37 °C in a 10% CO_2 atmosphere. Half-medium changes were performed twice per week with DMEM containing 10% horse serum. DHA working solutions were prepared in DMSO and kept under N_2 atmosphere to prevent oxidation and aliquoted. DHA was administered at 20 µM during all half-medium changes.

Cytochemical Studies

Immunostaining of cultured hippocampal neurons for synaptic marker analyses was performed using standard procedures at 14 div. Following fixation with 4% PFA and block, neurons were stained with primary antibodies diluted in 3% fetal bovine serum (FBS) and 0.01% Triton-X 100 in PBS, and incubated overnight at 4 °C. Secondary antibodies were diluted in 3% FBS and applied for 4 h at 4 °C. Neuronal cultures were stained with mouse monoclonal antibodies against Bassoon (AssayDesigns Cat# VAM-PS003F, RRID:AB_2313991; 1:500), polyclonal antibodies raised in rabbit against Homer 1 (Synaptic Systems Cat# 160003, RRID:AB_887730; 1:600) and vGAT (Synaptic Systems Cat# 131003, RRID:AB_887869; 1:500), polyclonal antibodies raised in guinea pig against vGlut1 (Millipore Cat# AB5905, RRID:AB_2301751; 1:500), and polyclonal antibodies raised in mouse against MAP2 (Millipore Cat# MAB3418, RRID:AB_94856; 1:1000). Secondary immunostaining was performed with anti-IgG2a Alexa 488 (Thermo Fisher Cat# A21240, RRID:AB_2535809), anti-rabbit Alexa 555 (Thermo Fisher Cat# A21428, RRID:AB_2535849), and anti-IgG1 Alexa 647 (Thermo Fisher Cat# A-21131, RRID:AB_2535771) antibodies (all at 1:500). Coverslips were washed in PBS and mounted with Aqua/PolyMount (Fisher, NC9439247). Confocal microscopy was performed on a Leica TCS SP8. Images were acquired with an ACS APO ×63 oil lens with 1.4 NA, using the same settings for each condition. Secondary and tertiary dendrite segments between 20–50 µm length were selected for analysis. During image acquisition and analysis, the researcher was blind to the condition. Images were analyzed using ImageJ using a custom written automated script (Dr Lai Ding, NeuroTechnology Studio and Program for Interdisciplinary Neuroscience, Brigham and Women’s Hospital). The annotated image analysis macro is available at https://github.com/becarbone/dendriteAnalysis.

Dendrite complexity was analyzed using hippocampal neurons prepared as described above. Neurons were transfected at 10 div with 500 ng/coverslip of a pCAGGS-GFP vector (a gift from Dr Nenad Sestan, Yale University) using Lipofectamine

Downloaded from https://academic.oup.com/cercor/advance-article-abstract/doi/10.1093/cercor/bhz083/5480315 by Tufts University user on 29 April 2019

LTX (Thermo Fisher Scientific Cat# 15338-100), and fixed at 21 div. For parallel analysis of neuronal cell body density, cultures were immunostained with mouse antibodies against NeuN (Millipore Cat# MAB377, RRID:AB_2298772; 1:500) followed by secondary staining using anti-IgG1 Alexa 568 (Thermo Fisher Scientific Cat# A-21124, RRID:AB_2535766). Coverslips were mounted with Vectashield (Vector Labs, VWR Cat# 101098-050). Dendrites of GFP-filled neurons were selected in ImageJ with the "Simple Neurite Tracer" (Longair et al. 2011). The GFP channel was adjusted to grayscale, contrast was enhanced for greater visibility of small processes, and dendrites were traced from the soma and annotated as primary/secondary/tertiary. Tracings were analyzed in ImageJ using the Sholl analysis plugin (Ferreira et al. 2014).

Immunostaining of neurons cultured on MEA chips was performed at 14 div. Following fixation with 4% PFA and blocking, primary antibodies were applied in 1% BSA, 2% goat serum, and 0.05% TWEEN20 (Sigma-Aldrich). Cultures were probed overnight at 4 °C with monoclonal antibodies raised in rabbit against synapsin-1 (Cell Signaling Technology, clone D12G5 Cat# 5297, RRID:AB_2616578; 1:200) and monoclonal antibodies raised in mouse against tubulin beta-III (Sigma-Aldrich, clone 2G10 Cat# T8578, RRID:AB_1841228; 1:750). Nuclei were detected by co-staining with the DNA-dye Hoechst/Bisbenzimide (Sigma-Aldrich Cat# 94403; 1 µg/ml). Secondary antibody staining was performed with goat-anti-rabbit Alexa 488 (Thermo Fisher Scientific Cat# A27034, RRID:AB_2536097) and anti-mouse Alexa 594 (Molecular Probes Cat# A-21044, RRID:AB_141424) for 1 h at room temperature (both at 1:500). Cells were embedded with ProLong Gold Antifade Mountant (Thermo Fisher Cat# P36930) and images acquired with an upright fluorescence microscope (Nikon Eclipse TE200, Nikon).

MEA Recordings of Cultured Neurons

MEAs were performed as described (Gramowski-Voss et al. 2015; Feng et al. 2018). Briefly, recordings were executed with a Maestro system (Axion Biosystems, Atlanta, GA, USA) providing ×1200 amplification, sampling at 12.5 kHz, filtering, and spike detection, delivering whole channel neuronal spike data. For extracellular recordings, MEA cultures were maintained at 37 °C and a pH of 7.4 through a continuous filtered and humidified airflow with 10% CO_2. Recordings were performed in DMEM with 10% horse serum. The network activity was recorded for at least 1 h. Unit separation was performed using Spike Splitter (NeuroProof GmbH, Rostock, Germany) based on different waveform shapes yielding up to 2 units per electrode. A unit represents the activity originating from 1 recorded neuron. Units were separated at the beginning of the recording. The stable activity phase of the last 30 min was analyzed. Action potentials (spikes) were recorded as spike trains, which are clustered in so-called bursts. Bursts were quantified via direct spike train analysis using the standard interspike interval (ISI) method in NPWaveX (NeuroProof). Bursts were defined by these parameters: maximum ISI to start a burst, 40 ms; minimum ISI to end a burst, 200 ms; minimum interval between bursts, 100 ms; minimum duration of burst, 10 ms; and min number of spikes in a burst, 5.

Functional parameters measured using MEA recordings included descriptors of General Activity and Burst Structure as follows. General Activity parameters: burst rate -number of bursts per minute, averaged over all units recorded. Event rate -number of events per minute. One event was defined as a synchronous burst activity of at least 50% of all units within 300 ms. Burst Structure parameters: percentage of spikes in bursts is the fraction of spikes within bursts in relation to all spikes recorded within the experimental episode. Standard deviation of the mean (SD) parameters reflect the temporal activity pattern for each unit, representing the regularity of periodic events. They are a measure for oscillatory behavior with larger values indicating a higher variability and complexity. SD values were averaged across the network. Burst rate SD -standard deviation of number of bursts per minute, indicating the variability of burstiness of units within experimental episodes. Burst period SD -SD of burst period, reflecting the variability of the distance between consecutive events.

In Vivo Visually Evoked Potential Recordings

Recordings were performed at P28/29 or at P35, after daily oral administration of DHA or vegetable oil vehicle from P1. Mice were implanted with light titanium headplates 7 days prior to visually evoked potential (VEP) recordings. Three to four days after headplate implantation, animals were habituated on the recording set-up by fixing the headplate to the headplate holder and allowing the animal to walk or run on the air-suspended styrofoam ball (Niell and Stryker 2010). Habituation was performed in daily 15-min long sessions for 2–3 consecutive days. On the day before recording, animals were anesthetized, and a small craniotomy (approximately 300 × 300 µm) was performed over the binocular visual cortex of 1 hemisphere. The craniotomy location was 2.0–2.5 mm lateral from the midline and 0.5 mm anterior to lambda. The next day, animals were fixed to the headplate holder via their headplate and VEP recordings were performed on a set-up based on a spherical treadmill design (Dombeck et al. 2007). VEPs were recorded through the created small craniotomy by inserting a linear, 15-µm thick 16-channel electrode (model A1x16-5 mm-50-177-A16, Neuronexus, Ann Arbor, MI) into the binocular visual cortex. Habituation and recordings were performed during the light cycle (7AM-8PM). Visual stimuli were presented as described below.

Visual Stimulation

During VEP recordings, mice were presented with random sinusoidal gratings differing in frequency and direction. The display was placed 14 cm in front of the animal and centered on its midline, thereby covering 81 ×86° of the visual field. Gratings were defined by the frequency, that is, the number of pairs of black-and-white stripes or cycles, within 1 degree of visual angle. For comparative measurements of contralateral and ipsilateral responses, white light was presented using a customized LED light source. The region of the visual field yielding VEPs with a contralateral to ipsilateral ratio between 1.4–3.3 established for each electrode penetration to confirm binocular visual cortex (V1b). Gratings were presented to each eye one at a time while the other eye was covered with electrical tape protruding from the headpost to the tip of the mouse's nose. This experimental design was modified and adapted from previous descriptions of VEPs recordings in mice (Porciatti et al. 1999; Niell and Stryker 2008).

Downloaded from https://academic.oup.com/cercor/advance-article-abstract/doi/10.1093/cercor/bhz083/5480315 by Tufts University user on 29 April 2019

VEP Analysis

Visual acuity was determined by linear regression based on VEP amplitude from 0.15, 0.30, and 0.60 Cpd (Cycles per degree). Amplitude was measured as the peak of the VEP prior to the negative-going component to the trough. Noise response amplitudes for each mouse were obtained during recordings. Visual acuity was determined as the Cpd value where noise intersected the linear regression on the *x*-axis. A minimum of 5 VEPs was used per direction and frequency per animal, with no maximum number of VEPs (some more than 25). A minimum of 13 min was used to obtain this data, again with no maximum time. Recording durations differed due to running, with some lasting approximately 30 min. Control mice showed the expected visual acuity around 0.5 Cpd (Porciatti et al. 1999).

Animal Information

All animal procedures undertaken in this study to generate immunochemistry data have been approved by the Tufts University Institutional Animal Care and Use Committee and are in compliance with NIH guidelines. For MEA experiments, neural tissue was prepared from pups according to the EU Directive 2010/63/EU on the protection of animals used for scientific purposes (certification file number 7221.3±2) and no animal experiments were performed in accordance with the German Animal Protection Act §7/2 (Tierschutzgesetz). These mice were sacrificed by cervical dislocation according to the German Animal Protection Act §4.

Data and Statistical Analyses

All quantitated analyses were performed with the researcher blind to the condition. Statistical analyses of normally distributed data were performed in GraphPad Prism 7.0 (GraphPad Inc., La Jolla, CA) using Student's t-test or 1-way ANOVA with post-hoc comparison as indicated in the text and legends. All data are reported as mean, with errors corresponding to the standard error of the mean. $^{*}P < 0.05$; $^{**}P < 0.01$; $^{***}P < 0.001$.

Results

Increased Abundance of Excitatory Synapses in the Visual Cortex after DHA Administration

Aiming to determine DHA effects on synapse number during postnatal cortical development, we selected a sensory area due to their stereotypical development and chose the visual cortex V1. C57Bl/6 wild-type littermate mice received daily from the day after birth (P1) by oral delivery 300 mg DHA/kg/day, a dose that increases DHA abundance in rodent cortex and hippocampus (Gamoh et al. 1999). Control mice received an equivalent volume of the vegetable oil that was used as diluent. The amount of DHA that treated mice received is estimated to be ~6-fold higher than what control mice take in via breast milk (see Materials and Methods). Following daily delivery of DHA or vegetable oil, mice were perfused at P35, when the visual cortex of mice has completed maturation and reached a visual acuity plateau (Huang et al. 1999).

We performed immunostaining for the excitatory postsynaptic scaffold protein Homer 1 in brain sections containing the visual cortex (Fig. 1A). Analysis of single optical sections of layer IV of V1 determined that the intensity of immunodetected Homer 1 was 32 ± 15% higher in DHA-treated mice than in control mice (Student's t-test, $P = 0.035$; for additional statistical information, see figure legends; Fig. 1B). Immunohistochemical staining for the excitatory presynaptic marker vGlut1 was additionally performed (Fig. 1C). DHA administration increased the fluorescence intensity of this synaptic vesicle protein by 22 ± 6% (Student's t-test, $P = 0.0125$) compared with control animals (Fig. 1D). Aiming to measure DHA effects on the number of presynaptic sites, we applied the threshold-independent, machine–learning-based Intellicount algorithm (Fantuzzo et al. 2017). Analysis of single optical sections showed that DHA administration increased the density of vGlut1 puncta in layer IV of V1 modestly but significantly by 9.8 ± 2.5% (Student's t-test, $P < 0.001$) over control mice (Fig. 1E,F). This approach also measured an increase in the staining intensity of vGlut1 puncta after DHA treatment by 12.0 ± 4.7% (Student's t-test, $P = 0.011$). Together, these results demonstrated an increase in the number of excitatory specializations in the cortex of DHA-supplemented mice.

DHA Promotes the Number of Presynaptic and Postsynaptic Specializations in a Dose-Dependent Manner

DHA effects on synapse development were further defined in cultures of dissociated hippocampal neurons that were treated with DHA over a 60-fold concentration range, starting at 4 days in vitro (div; Fig. 2A). Neuronal density at 14 div was analyzed by immunostaining for the neuronal nuclei marker NeuN and no effect of DHA on the number of neurons was observed (data not shown). Quantitative immunocytochemical analysis of presynaptic and postsynaptic specializations was performed at 14 div by immunostaining for the active zone protein Bassoon and the excitatory marker Homer, respectively. Unbiased, semi-automated image analysis demonstrated that DHA increased the number of presynaptic, Bassoon-positive specializations along MAP2-positive dendrites compared with vehicle-treated control neurons if neurons were treated with 4 µM DHA or higher concentrations (Fig. 2B). DHA in addition elevated the density of excitatory, Homer-positive postsynaptic sites with the same dose dependency (Fig. 2C). DHA treatments lower than 4 µM had no effect. Treatment with 16 µM DHA, the highest dose tested, increased the density of presynaptic Bassoon and postsynaptic Homer puncta substantially by 48 ± 10% ($P < 0.0001$) and 55 ± 14% ($P = 0.001$), respectively, compared with vehicle-treated control neurons prepared in parallel.

DHA effects on excitatory versus inhibitory synapses were compared by treating hippocampal neurons as above, followed by co-immunostaining for the excitatory presynaptic marker vGlut1 and the inhibitory presynaptic marker vGAT (Fig. 2G). DHA treatment at 4 µM increased the number of vGlut1 puncta along MAP2-positive dendrites by 35 ± 15% ($P = 0.025$), in agreement with its effect on the excitatory postsynaptic marker Homer (Fig. 2H). In addition, the density of vGAT-positive inhibitory presynaptic sites, which are less abundant in hippocampal neurons, was increased upon DHA treatment by 38 ± 16% ($P = 0.024$; Fig. 2I). The more pronounced increase in Bassoon puncta density (Fig. 2B) likely reflected the combined recruitment of vGlut1- and vGAT-positive presynaptic sites to dendrites. Higher DHA amounts therefore robustly promoted the number of excitatory and inhibitory synaptic sites.

Downloaded from https://academic.oup.com/cercor/advance-article-abstract/doi/10.1093/cercor/bhz083/5480315 by Tufts University user on 29 April 2019

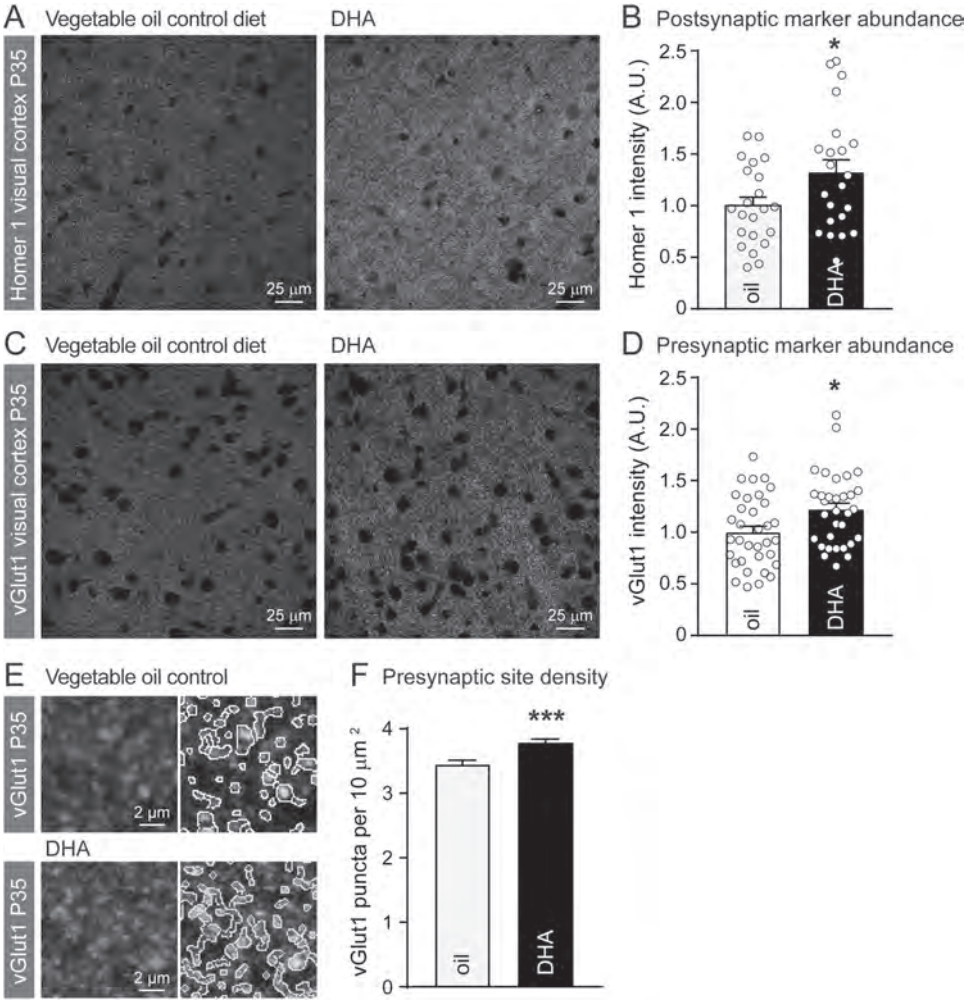

Figure 1. Increased abundance of excitatory synaptic sites in the visual cortex of DHA-treated mice. (*A*) Homer 1 immunostaining in binocular visual cortex V1, layer IV of P35 mice whose diet had been supplemented daily from P1 with the vehicle vegetable oil as control (left) or DHA (right). Representative single optical sections obtained by confocal microscopy are shown; (*B*) Quantification of Homer staining intensity from single optical sections as in (*A*). $N = 22$ optical sections from 3 DHA-treated mice with 7/7/8 sections per mouse, and $N = 22$ optical sections from 3 control mice with 8/6/8 sections per mouse. (*C*) vGlut1 immunostaining in binocular visual cortex V1, layer IV of P35 mice treated as in (*A*). Representative single optical sections are shown; (*D*) Quantification of vGlut1 staining intensity from single optical sections as in (*B*). $N = 32$ optical sections from 3 DHA-treated mice were comprised of 12/8/12 sections per mouse, and $N = 34$ optical sections from 3 control mice corresponded to 12/10/12 sections per mouse; (*E*) Representative vGlut1 immunostainings obtained as in (*C*) before (left) and after (right) algorithm processing to identify synaptic puncta marked by white outlines; (*F*) Analyses of images processed as in (*E*) determined that DHA increased vGlut1 puncta density. $N = 102$ images DHA, 89 veg. oil control from 3 mice per condition.

Elevated Amounts of DHA Increase Synapse Size and the Number of Presynaptically and Postsynaptically Aligned Sites

Synapse size is an additional parameter relevant for synapse maturation, and we analyzed presynaptic Bassoon-positive and postsynaptic Homer-positive sites at 14 div. DHA treatment at the highest concentration of 16 µM increased the size of presynaptic (Fig. 2*D*) and postsynaptic specializations (Fig. 2*E*) by $26 \pm 3\%$ and $18 \pm 3\%$ ($P < 0.0001$ each), respectively, compared with vehicle-treated control neurons.

We next asked whether DHA increases the number of contacts where presynaptic and postsynaptic sites align with each other. We addressed this by measuring the extent to which presynaptic Bassoon-positive sites were co-localized with postsynaptic sites positive for Homer along MAP2-positive dendrites. This determined that DHA treatment at 4 µM or higher elevated the density of aligned presynaptic and postsynaptic specializations, and DHA treatment at 16 µM increased the number of Homer puncta aligned with Bassoon puncta by $58 \pm 14\%$ ($P = 0.0003$) compared with controls (Fig. 2*F*). This supported that the additional presynaptic and postsynaptic specializations formed in presence of DHA are properly assembled into synapses.

Dendritic Arborization Is Increased by DHA Treatment

Extending our analysis of DHA effects on morphological parameters of neuronal maturation, we analyzed the complexity of dendritic arbors in hippocampal neurons (Fig. 3*A*). Neurons were treated with vehicle control or 4 µM DHA and sparsely transfected with GFP as volume fill. At 14 div, we performed a Sholl analysis of the number of intersection of

Downloaded from https://academic.oup.com/cercor/advance-article-abstract/doi/10.1093/cercor/bhz083/5480315 by Tufts University user on 29 April 2019

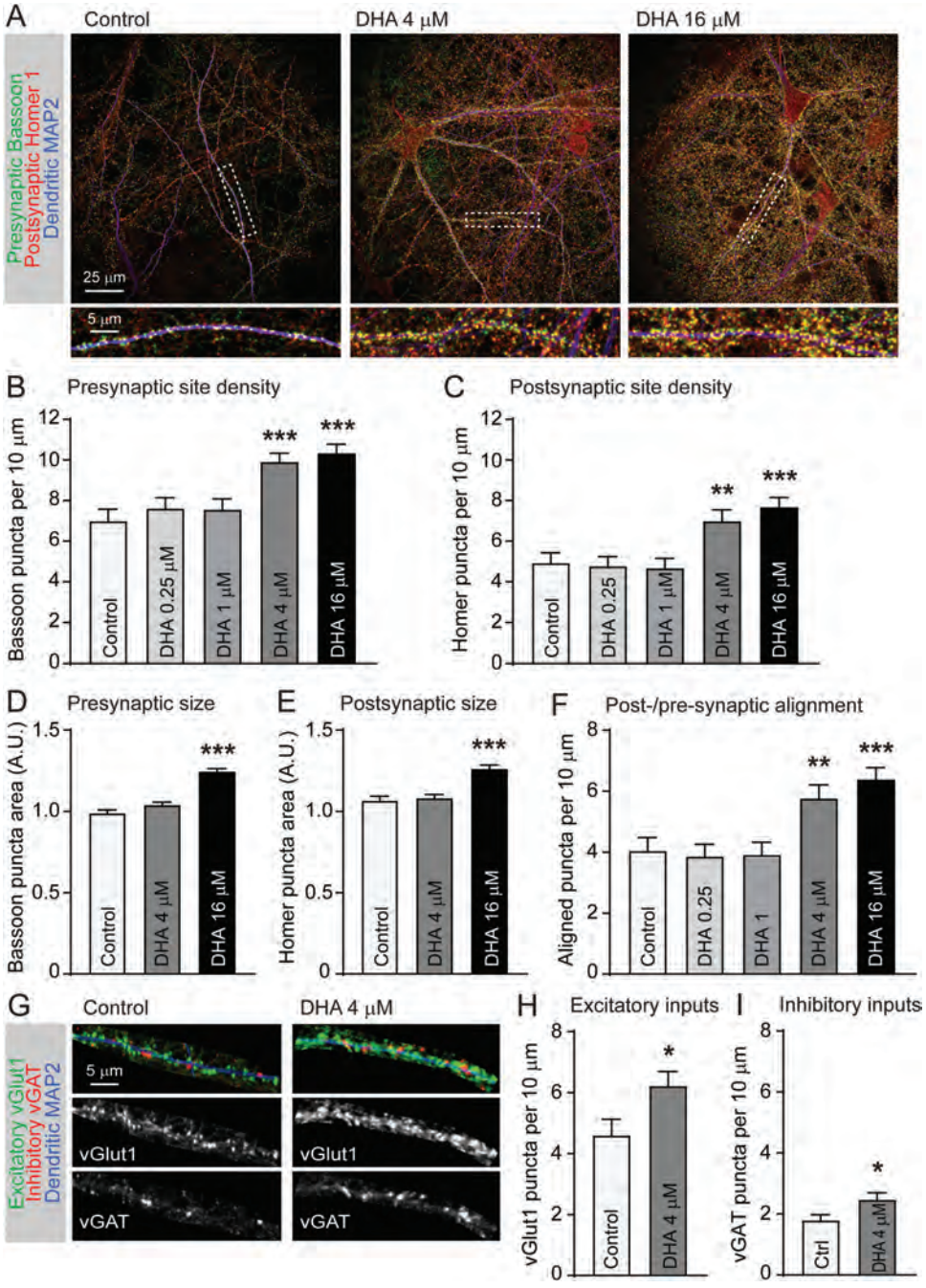

Figure 2. DHA promotes the development of presynaptic and postsynaptic specializations. (*A*) Dissociated hippocampal neurons were treated with the vehicle DMSO as control or DHA at 4 or 16 μM as indicated on top. Immunostaining for the presynaptic marker Bassoon (green), the excitatory postsynaptic marker Homer 1 (red), and the dendrite marker MAP2 (blue) was performed at 14 days in vitro (div). Top, representative overview images obtained by confocal microscopy. Bottom, panels show enlarged dendritic segments boxed on top; (*B*,*C*) Quantification of images as in (*A*) determined that DHA treatment of neurons at 4 or 16 μM but not lower doses increased the density of presynaptic specializations positive for Bassoon (*B*) or excitatory postsynaptic sites marked by Homer (*C*) per length of dendritic segment. Lower DHA amounts have no effect. $N = 70$ dendritic segments (DMSO control), 66 (DHA 0.25 μM), 66 (1 μM), 65 (4 μM), and 70 (16 μM). Data from 4 independent experiments. One-way ANOVA with Tukey's multiple comparison test. $^{**}P < 0.01$, $^{***}P < 0.001$; (*D*,*E*) Quantification of images as in (*A*) showed that DHA treatment of neurons at 16 μM but not lower doses increased the size of presynaptic Bassoon-positive specializations (*D*) and of excitatory postsynaptic sites positive for Homer (*E*). N of Bassoon puncta = 1681 (DMSO control), 1737 (DHA 0.25 μM), 1599 (1 μM), 2241 (4 μM), and 2427 (16 μM). N of Homer puncta = 1188 (DMSO control), 1095 (DHA 0.25 μM), 1003 (1 μM), 1578 (4 μM), and 1797 (16 μM). Data from 4 independent experiments. One-way ANOVA with Dunnett's multiple comparison test; (*F*) Quantification of images as in (*A*) determined that DHA treatment of neuron at 4 or 16 μM but not lower doses increased the density of sites where excitatory postsynaptic sites are co-localized with presynaptic sites. One-way ANOVA with Dunnett's multiple comparison test. $^{**}P < 0.01$, $^{***}P < 0.001$; (*G*) Dendritic segments of hippocampal neurons treated with DMSO control (left) or 4 μM DHA (right). Quantitative immunostaining for the excitatory presynaptic marker vGlut1 (green) and inhibitory presynaptic vGAT (red) was performed at 14 div. Top, merged images. Bottom, individual channels; (*H*,*I*) Quantification of images as in (*G*) showed that DHA treatment increased the density of sites positive for vGlut1 (*H*) and vGAT (*I*). N of dendritic segments = 36 per condition. Data from 2 independent experiments. Student's unpaired t-test $^{*}P < 0.05$.

Downloaded from https://academic.oup.com/cercor/advance-article-abstract/doi/10.1093/cercor/bhz083/5480315 by Tufts University user on 29 April 2019

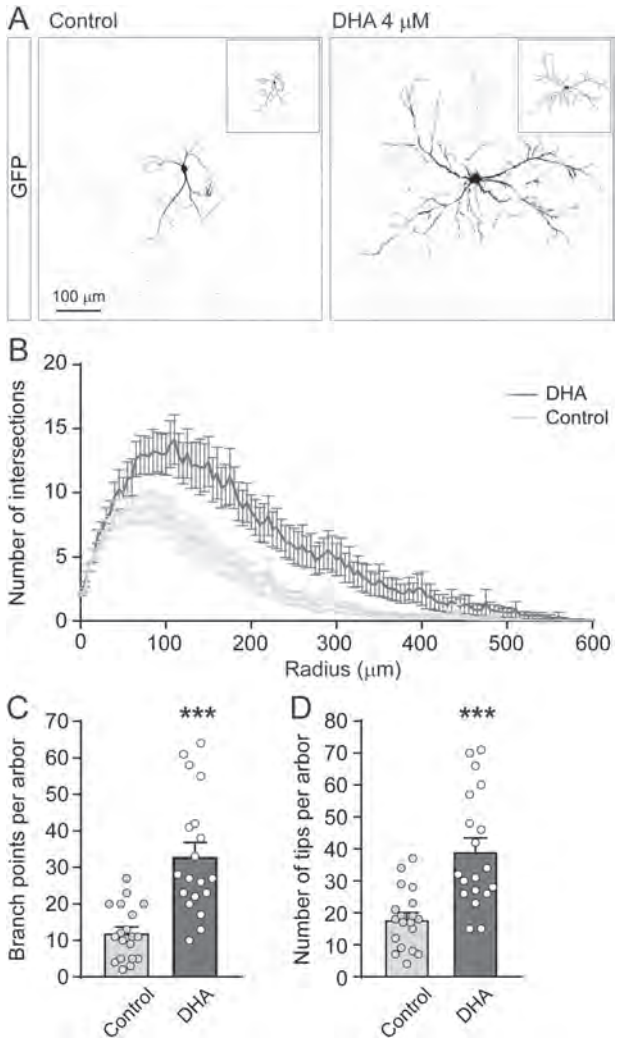

Figure 3. Dendrites are more complex upon DHA treatment. (*A*) Images show dissociated hippocampal neurons at 14 div sparsely expressing the volume marker GFP to visualize dendritic arbors. Neurons were treated with DMSO vehicle control (left) or 4 µM DHA (right). Insets show dendrite tracings as used for quantification; (*B*) Sholl analysis of dendritic arbors visualized as in (*A*) determined increased complexity upon DHA treatment; (*C*,*D*) Analysis of images as in (*A*) showed an increase in branch points (*C*) and number of tips (*D*) per dendritic arbor. (*B*–*D*) $N = 19$ neurons per condition. Data from 2 independent experiments. Student's unpaired t-test $^{***}P < 0.001$.

dendritic trees with a series of concentric spherical shells (Sholl 1953). This confirmed the visual impression that DHA treatment robustly promoted the complexity of dendritic arbors [2-way ANOVA, $P = 0.0017$ for treatment condition, $F(1, 36) = 11.44$; Fig. 3B]. In agreement, branch points per dendritic arbor were more abundant by 18 ± 3% (Student's t-test, $P < 0.0001$), and the number of dendritic tips was increased by 18 ± 3% ($P < 0.0001$; Fig. 3C,D). These changes were driven by a 3.5-fold increase in the number of tertiary dendrites, extending total dendritic arbor length from 2100 ± 332 µm (control) to 4411 ± 585 µm (DHA) (Student's t-test, $P = 0.0015$; $N = 19$ neurons each).

DHA Supports Maturation of Neuronal Network Connectivity

Aiming to measure DHA effects on functional neuronal connectivity, we applied microelectrode arrays (MEA) for extracellular recording of action potentials of cultured neurons (Supplementary Fig. 1). MEAs can elucidate synaptic modulation and activity characteristics of networks and have been used to investigate neuronal development (Gramowski-Voss et al. 2015; Odawara et al. 2016; Bader et al. 2017) and to screen pharmacological agents (Gramowski et al. 2006). This approach measures not only spontaneous activity patterns but also allows one to deduce network properties.

We performed these experiments in cortical neurons to scale up the cultures as required for MEA chips. Neurons from mouse frontal cortex were grown on MEAs and subjected to DHA versus control treatment. These cultures were chosen as their well-defined maturation profile on MEAs (see references above) enabled testing to what extent DHA modulated the establishment of network properties. Activity-describing parameters were calculated based on spike trains (time stamps of action potentials), which can be divided into different parameter categories (Bader et al. 2017). Using multi-well MEAs for longitudinal recording from 6–20 div, we tracked these network properties (Fig. 4A) and structures of spike bursts (Fig. 4B). General Activity descriptors represent overall network activity parameters such as burst rate. Burst Structure parameters describe the internal structure of bursts and rhythm of spikes in bursts. Network connectivity parameters indicate the regularity and oscillation of events, defined as periods of synchronous burst activity. They are represented by the standard deviations (SDs) associated with main General Activity and Burst Structure parameters during events, with higher SD values indicating more variably patterned activity and burst structure.

Control cultures reached a plateau in functional development by 20 div, as described (Ito et al. 2013). Their spontaneous network activity progressively increased as measured for burst rates (Fig. 4C) and for periods with synchronous burst events (Fig. 4D). Spikes in control cultures were also increasingly more clustered within bursts as the network matured to 20 div (Fig. 4E). Bursts in addition exhibited progressively higher variability during development as reflected by the gradual increase in the SD of burst rates over time, indicating more complex oscillatory activity patterns (Fig. 4F). The variation of burst period length between control neurons in the network decreased over time (Fig. 4G). This lower value of burst period SD is a measure for lower variability in event period lengths and reflects higher event synchronicity. These results showed a progressive increase in synchronized connectivity as control neurons matured.

Functional effects of DHA were longitudinally followed using multi-well MEAs, and cultured neurons were recorded from 6–20 div and compared with control cultures. A dose of 20 µM DHA was chosen to achieve strong synaptogenic effects (see Fig. 2, and data not shown). DHA significantly enhanced maturation-relevant network parameters. Addition of DHA increased overall activity at 14–16 div (Fig. 4C,D). DHA continued to further increase activity at 20 div as indicated by higher burst rate and higher rate of synchronized population bursts termed events. Further, DHA modestly but significantly promoted the establishment of burst structures and reduced the clustering of spikes in bursts, which resulted in more complex and variable bursting (Fig. 4E). This enhancement was also seen

Downloaded from https://academic.oup.com/cercor/advance-article-abstract/doi/10.1093/cercor/bhz083/5480315 by Tufts University user on 29 April 2019

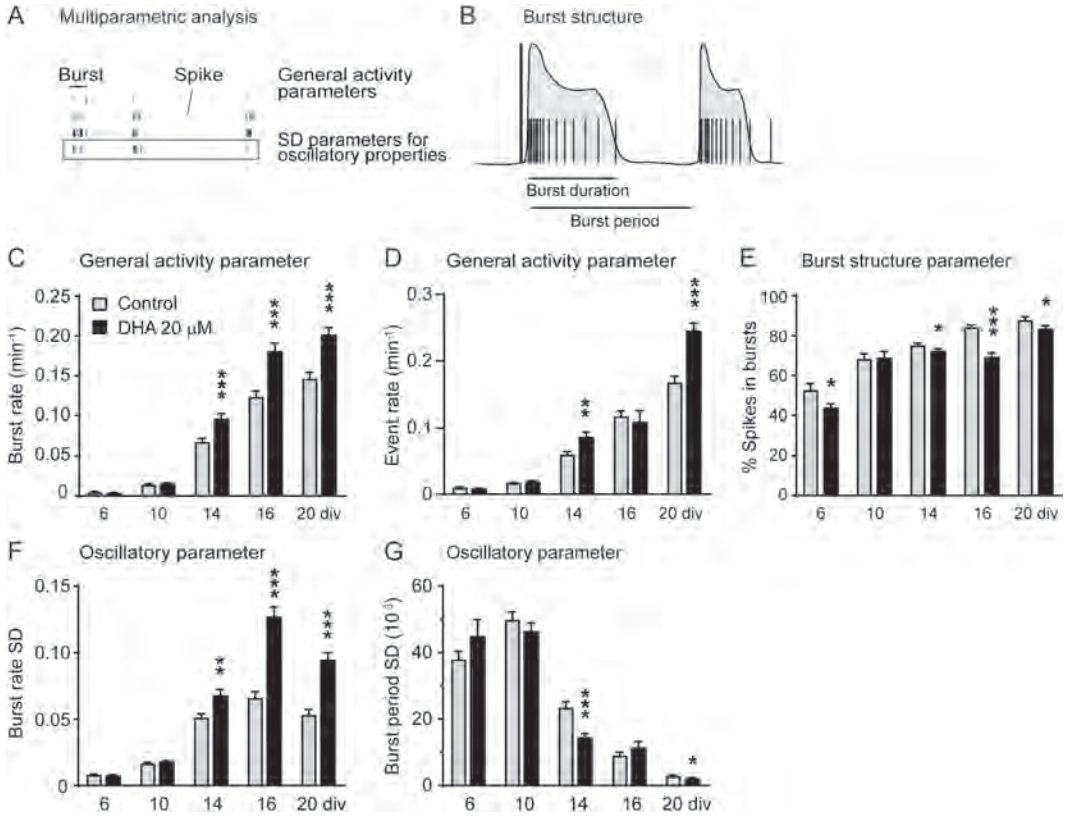

Figure 4. Functional maturation of cortical neuronal networks is promoted by DHA. (*A*) The panel shows raw data from a spike raster plot recorded from cortical neurons cultured on mircoelectrode arrays. Categories of activity parameters are indicated; (*B*) Diagram of 2 schematized bursts outlining burst structure parameters extractable from the recordings; (*C–E*) General activity parameters of burst rate (*C*), event rate (*D*), and fraction of spikes occurring within bursts (*E*). Parameters show the developmental maturation of functional network connectivity between 6–20 div as indicated for the DSMO vehicle control condition (gray bars). DHA significantly accelerated maturation (black bars); (*F,G*) Network and oscillation properties of burst rate standard deviation (SD) (*F*) and burst period SD (*G*). Student's unpaired t-test $^{*}P < 0.05$; $^{**}P < 0.01$; $^{***}P < 0.001$.

for oscillation-relevant properties. Here, DHA promoted the increase in diversity of burst rates as neurons matured (Fig. 4F) and supported the developmental decrease in the variation of burst event periods (Fig. 4G). DHA hence promoted physiological parameters of network maturation and the complexity of activity patterns.

DHA Supplementation Promotes Visual Acuity in Maturing Animals

Does DHA administration have functional effects on neuronal networks as they develop in vivo? To test this, we analyzed the visual cortex. Our approach was based on recording VEPs from the binocular zone of V1 of awake mice that were presented with grated visual patterns. VEPs represent the integrated response of a population of neurons and have been used to measure acuity and other parameters of vision in a number of mammals, including rats and mice (Birch and Jacobs 1979; Huang et al. 1999). Mice open their eyes around P14 and visual acuity progressively increases thereafter, reaching a plateau by P35 when acuity has improved 3–4-fold (Huang et al. 1999). This pronounced and stereotypic increase in the visual acuity of mice provided the opportunity to measure to what extent DHA affects the function of the maturing cortex at different developmental points.

Wild type (WT) Littermate mice received daily 300 mg DHA/kg/day or the equivalent volume of vegetable oil as vehicle control from P1 as for our immunohistochemical experiments (Fig. 1). Another group of mice received no dietary supplementation and stayed in the home cage to control for possible effects of the daily handling during compound delivery on cortical maturation. No effect of DHA or vegetable oil supplementation on healthy body growth was observed (Fig. 5A). We selected 3 time points for functional in vivo analyses and first tested animals at P28, when visual acuity in wild-type mice is starting to reach adult levels (Huang et al. 1999). Recordings of VEPs were obtained from animals that were allowed to freely run on a ball that floats on air, known as a spherical treadmill (Dombeck et al. 2007; Fig. 5B). Prior to the recordings, custom-made headposts were implanted to the skull and mice were habituated mice to the set-up. On the recording day, a small craniotomy was made over binocular V1 (less than 0.5 mm in diameter), and mice were mounted via their headpost atop the ball. A multichannel electrode was inserted in the binocular zone of V1, and recordings were obtained from all cortical layers while sinusoidal gratings were presented to each eye individually. Gratings were presented randomly with respect to frequency and direction. Low frequency stimulation at 0.15 Cpd at full contrast elicited highest VEP amplitudes in control mice that received vegetable oil, as previously described (Huang et al. 1999; Porciatti et al. 1999; Cancedda et al. 2004). VEP amplitudes

Downloaded from https://academic.oup.com/cercor/advance-article-abstract/doi/10.1093/cercor/bhz083/5480315 by Tufts University user on 29 April 2019

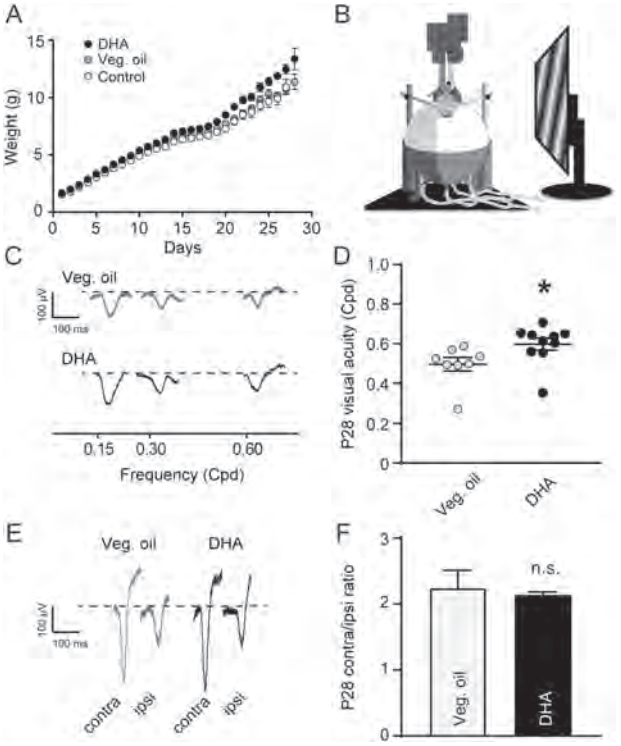

Figure 5. DHA supplementation increases visual acuity in young animals. (*A*) Vegetable oil as vehicle control or DHA were administered orally daily from P1. Administration of vegetable oil (gray) or DHA (black) did not alter normal weight gain compared with untreated, non-handled cage control mice (white). $N = 37$ mice (veg. oil), 32 (DHA), 30 (cage control); (*B*) Model of the spherical treadmill set-up for in vivo recordings from awake mice; (*C*) Representative VEP waveforms recorded at P28/29 from the binocular zone of the visual cortex of mice, layer IV, while mice viewed gratings of frequencies at the indicated Cpd. Amplitudes of VEPs were calculated by measuring the distance from the first peak (marked by the horizontal line) to the trough of the VEP. The correct layer was determined by identifying the electrode channel in which the greatest contralateral response amplitude was recorded; (*D*) Daily DHA administration from birth increased visual acuity at P28/29. Visual acuity was determined by creating a linear regression for each animal's response to the specific frequencies of sinusoidal gratings presented. Control mice exhibited the expected acuity around 0.5 Cpd (Porciatti et al. 1999); (*E*) Representative VEP waveforms recorded in layer IV upon white light flash stimulation of either the contralateral or ipsilateral visual cortex; (*F*) Contralateral to ipsilateral VEP amplitude ratios were recorded from layer IV of the binocular zone at white light stimulation. DHA did not affect baseline responses as amplitudes of stimulated contrastimulated and unstimulated ipsilateral cortex had the same ratio as controls. $^{*}P < 0.05$, $^{**}P < 0.01$, $^{***}P < 0.001$; error bars indicate SEM. (*D*,*F*) $N = 8$ veg. oil control mice, $N = 10$ DHA.

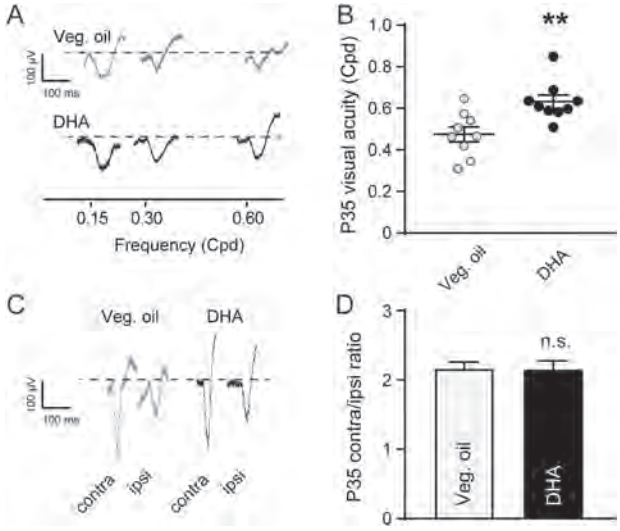

Figure 6. Visual acuity is elevated by DHA in the matured visual cortex. (*A*) Vegetable oil or DHA were administered daily from P1 and recordings were performed at P35. The panel shows representative VEP waveforms recorded from the binocular zone of the visual cortex as in Figure 5C; (*B*) Visual acuity was increased at P35 after DHA administration. Recordings were performed as in Figure 5D; (*C*) Representative VEP waveforms recorded at white light stimulation from layer IV of the binocular zone of either the contralateral or ipsilateral visual cortex; (*D*) DHA did not change the contralateral to ipsilateral VEP amplitude ratio recorded as in (*C*). $^{**}P < 0.01$; error bars indicate SEM. (*B*,*D*) $N = 9$ veg. oil control mice, $N = 9$ DHA.

progressively decreased with increased frequency of gratings (Fig. 5C). The daily handling of mice during oral supplement administration did not affect visual cortex maturation as acuity was not different between mice that received vegetable oil or that remained in the home cage (data not shown).

Mice that received DHA showed at P28 the expected peak visual responsiveness when stimulated with a grated pattern at 0.15 Cpd. VEP amplitudes appeared larger than in control mice, though (Fig. 5C). We determined visual acuity by creating a linear regression of VEP amplitudes for each animal. This measured an increase of visual acuity by 21% in DHA-supplemented mice compared with mice that had received vegetable oil alone (Fig. 5D; veg. oil control, mean visual acuity 0.496 ± 0.034 Cpd; DHA, 0.598 ± 0.031 Cpd; unpaired t-test, $P = 0.043$; $N = 8$ control mice, $N = 10$ DHA). In addition, we recorded VEPs elicited by full field flash stimulation. These VEPs reflect the integrity of rod and cone pathways to the cortex and are a measure of light sensitivity (Porciatti et al. 1999; Ridder and Nusinowitz 2006). DHA had no effect on flash VEPs (Fig. 5E), supporting that its administration did not alter the basic light sensitivity of cortical responses. We also tested whether DHA alters the extent to which mouse V1 is contralaterally driven, which is reflected in the high ratio of responses elicited through the contralateral eye to responses elicited through the ipsilateral eye (C/I ratio; Frenkel and Bear 2004). DHA supplementation did not affect the ratio and strength of contralateral and ipsilateral responses, as measured by VEPs elicited by both full field flash (Fig. 5F) and sinusoidal grating stimuli (veg. oil control C/I, 1.44 ± 0.28; DHA C/I, 1.70 ± 0.42; unpaired t-test, $P = 0.63$; $N = 8$ control mice, $N = 10$ DHA). DHA treatment hence did not affect gross development of central visual pathways. These results supported that DHA promotes the establishment of functional intracortical connectivity and visual processing.

DHA Administration Persistently Augments Visual Acuity

To address whether acuity continues to improve in DHA-supplemented mice, DHA or vegetable oil were administered from P1 to P35, and recordings were performed at that time. P35 was selected because V1 maturation is complete at this age (Huang et al. 1999). Mice in both groups exhibited the expected peak of visual acuity when stimulated with a pattern of 0.15 Cpd (Fig. 6A). Notably, DHA-supplemented mice reached 33% higher visual acuity at P35 compared with control mice (veg. oil control, mean visual acuity 0.475 ± 0.036 Cpd; DHA, 0.633 ± 0.031 Cpd; unpaired t-test, $P = 0.004$; $N = 9$ mice per group) (Fig. 6B).

Downloaded from https://academic.oup.com/cercor/advance-article-abstract/doi/10.1093/cercor/bhz083/5480315 by Tufts University user on 29 April 2019

Amplitudes and ratio of contralateral to the ipsilateral responses elicited by flash VEPs were indistinguishable (Fig. 6C,D), as at P28. In contrast to the effects of continued DHA administration, brief treatment of mice for only 7 days, from P28 to P35, did not elevate visual acuity at P35 (Supplementary Fig. 2). In addition, we measured whether an increase in visual acuity following continuous DHA treatment was also observed in fully mature mice at P45, when visual cortex maturation is complete and plasticity becomes restricted (Kuhlman et al. 2013). We found that mice supplemented with DHA from birth until P45 exhibited 41% higher visual acuity compared with their vegetable oil-receiving littermates (veg. oil control, mean visual acuity 0.509 ± 0.042 Cpd; DHA, 0.717 ± 0.012 Cpd; unpaired t-test, $P = 0.009$; $N = 3$ mice per group). Together, DHA increased visual acuity in young animals and even abolished the acuity plateau once their visual cortex has fully developed. These results provide evidence that DHA supplementation improves cortical maturation.

Discussion

We have here investigated roles of the dietary ω-3 fatty acid DHA in the development of synaptic connectivity and cortical function. Aiming to delineate effects in the maturing brain, we determined that daily DHA supplementation of mice from birth increased the abundance of excitatory synaptic specializations in the visual cortex. In agreement, DHA had robust effects on excitatory and inhibitory synaptic markers and dendrite complexity in cultured neurons. These effects included a DHA dose-dependent increase in the number and size of presynaptic and postsynaptic specializations, and these added sites were properly aligned. Functional connectivity was improved in presence of DHA as well, and this ω-3 fatty acid supported how patterned activity arises in developing neuronal networks. Furthermore, recordings from the visual cortex in maturing animals demonstrated beneficial effects of DHA on visual acuity, a measure of information processing in this cortical region.

DHA supplementation from birth increased the abundance of presynaptic and postsynaptic excitatory specializations in the visual cortex of mice as measured by immunohistochemistry. These in vivo data are consistent with DHA effects when administered to adult and aged rodents, which elevates in the hippocampus the number of dendritic spines, the postsynaptic sites onto which most excitatory synapses are formed, and enhances synaptic strength (Sakamoto et al. 2007; Connor et al. 2012). Correspondingly, synaptic fractions from DHA-deprived, adult mice have lower amounts of synaptic proteins (Sidhu et al. 2011; Lozada et al. 2017). Roles of DHA in modulating synapse number are evolutionarily conserved as it is required for normal synapse development in tectal neurons of *Xenopus laevis* tadpoles, which had fewer excitatory postsynaptic sites when mothers were deprived of DHA (Igarashi et al. 2015). Our results now demonstrate that providing DHA from birth can already promote synapse number.

Our cellular analysis in cultured neurons provided additional evidence that DHA treatment promotes the density and size of synaptic connections. Our results agree with and extend previous studies in dissociated neurons that reported increased presynaptic marker staining and elevated activity upon treatment with DHA (Cao et al. 2009; Kim et al. 2011a). Our finding that DHA increased the density of both excitatory and inhibitory synaptic sites indicates that while network connectivity is increased, it remains balanced. Indeed, the DHA-induced improvements in synaptic connectivity we measured using immunocytochemistry match the enhanced maturation of physiological network properties in presence of this ω-3 fatty acid as recorded using MEAs. Specifically, DHA elevated spike and burst activity, together with higher bursting strength and burst synchronization, and more complex oscillatory behavior. The DHA-dependent increase in synapse size may contribute to these effects as strength increases on the level of individual excitatory synapses are linked to enlargement of spines (Harvey and Svoboda 2007) and presynaptic bouton volume (Meyer et al. 2014). Our results point not only to networks being better connected in presence of DHA but also to more dynamic and tuneable neuronal communication.

These effects are complemented by higher dendrite complexity upon DHA treatment, a role that also appears conserved as tadpoles from DHA-deprived mothers have simplified dendritic trees (Igarashi et al. 2015). This ω-3 fatty acid therefore impacts multiple aspects of neuronal differentiation, and our result that it increases both synapse density per length dendrite and the cumulative length of dendritic segments supports that it substantially increases the total number of synaptic inputs per neuron. DHA treatment hence robustly promotes the potential for neuronal connectivity in maturing neurons.

We performed functional analyses of DHA in the maturing visual cortex. This region was chosen for 2 reasons, first, because the stereotypic postnatal maturation of sensory systems enables to readily discern treatment effects and second, because the analysis of neural responses to visual cues can identify distinctly cortical processing features (Espinosa and Stryker 2012). We used mice as they are a well-established model organism for vision research due to the conserved connectivity of the visual system compared with primates and the similarly prolonged postnatal development of visual acuity in mice (Prusky and Douglas 2003; Niell and Stryker 2008). Further, the functional maturation of the visual cortex in mice follows a pattern with little inter-individual variability, ensuring robust results (Freeman and Marg 1975; Fagiolini et al. 1994; Huang et al. 1999; Heimel et al. 2007). Our visual acuity recordings at P28, that is, 2 weeks after eye opening in mice, determined that DHA significantly promotes cortical input processing already at this stage. Maturation of the visual cortex is complete by P35, and our recordings at this later stage showed that continuous DHA supplementation improves visual acuity even after the visual cortex has developed. This is consistent with the beneficial effects of DHA supplementation on visual acuity in healthy infants (SanGiovanni et al. 2000; Birch et al. 2010). These results support that this ω-3 fatty acid promotes the postnatal establishment of cortical function.

How does DHA achieve its effects? The synaptic parameters we have measured in vitro are improved with different dose dependencies and elevating DHA amounts first increases synapse number before making them larger. This indicates that DHA engages mechanisms that are activated at select thresholds to promote different aspects of synapse development. The mechanisms through which this ω-3 fatty acid may support neuronal differentiation are complex (Salem et al. 2001; Kim et al. 2011a,b; Calder 2012). One pathway is provided by the DHA metabolite N-docosahexaenoylethanolamide that increases the number of excitatory presynaptic sites via its G-protein coupled receptor GPR110 (ADGRF1; Lee et al. 2016). Additional mechanisms include biophysical effects of DHA that render membranes more deformable (Manni et al. 2018)

Downloaded from https://academic.oup.com/cercor/advance-article-abstract/doi/10.1093/cercor/bhz083/5480315 by Tufts University user on 29 April 2019

and alter membrane fluidity and liquid-ordered domains (Hashimoto et al. 1999; Stillwell et al. 2005; Pinot et al. 2014). In addition, dietary DHA regulates gene expression, which involves activation of the nuclear retinoid X receptor (de Urquiza et al. 2000; Kitajka et al. 2002). Moreover, the effects we report for DHA in synaptic connectivity may involve brain-derived neurotrophic factor (BDNF). Dietary deficiency of DHA during brain maturation lowers brain BDNF amount across species and impairs BDNF signaling (Bhatia et al. 2011; Igarashi et al. 2015), while DHA supplementation of adult rodents is sufficient to increase BDNF (Wu et al. 2008). Given the roles of BDNF signaling in the formation and maturation of synapses (Huang and Reichardt 2001; Zweifel et al. 2005; Park and Poo 2013), this neurotrophin may in part underlie DHA effects. Interestingly, the growth factors BDNF and IGF-1 improve visual acuity in rodents similar to DHA in our study (Huang et al. 1999; Sale et al. 2004; Ciucci et al. 2007; Mardinly et al. 2016). Future work can investigate to what extent these signaling pathways are modulated by DHA.

The effects of DHA we report here occur during a key period of postnatal brain maturation. It has been assessed that the developmental stage of sensory cortices in mice at P28 approximately corresponds to human sensorimotor cortex at 15 months of age (Workman et al. 2013). In rodents and primates, synapses are formed at a fast pace preceding these periods. Synaptogenesis in the mouse cortex peaks during the second and third week after birth (Aghajanian and Bloom 1967; Micheva and Beaulieu 1996). In primates, rapid synaptogenesis occurs in the visual cortex until about 8 months of age, followed by input refinement and pruning (Huttenlocher et al. 1982; Rakic et al. 1986). Concomitantly, visual acuity in children modestly improves in the first 6 months and then steadily increases after 12 months of age until it plateaus at 5 years (Dobson and Teller 1978; Mayer and Dobson 1982). In agreement with a translational relevance of our results, continued DHA supplementation of healthy infants supports visual acuity (SanGiovanni et al. 2000; Birch et al. 2010) and improves visual impairments in preterm children (Molloy et al. 2012). DHA appears to act most potently during specific windows. DHA treatment for only 7 days up until P35, that is, after maturation of the visual cortex is mostly complete, did not improve visual acuity, though other aspects of cortical function may still be supported. Regarding visual acuity, this lack of an effect after temporary treatment differs from the strong benefits of DHA administration from birth at P28 and later. These results support that DHA is more effective when already provided during development, and its early administration may set the stage to further advance brain maturation. DHA may not only involve improved synapse development but also processes such as synaptic remodeling and input refinement, which can be tested in future studies.

The findings reported here agree with the important roles of polyunsaturated fatty acids in brain development and neurotransmission (Uauy et al. 2001; Innis 2008; Bazinet and Laye 2014) and support that the progressive synaptic membrane enrichment of DHA in the postnatal brain (Tulodziecka et al. 2016) is functionally relevant. These roles can be viewed in the context of the complex lipidome of the mammalian brain, especially of the human brain, and the dynamic lipid composition of synaptic membranes (Dotti et al. 2014; Bozek et al. 2015). DHA amounts fluctuate strongly with dietary intake and show higher variability than other long-chain polyunsaturated fatty acids in breast milk (Smit et al. 2002; Brenna et al. 2007). Steadily supplied dietary DHA may both increase and stabilize brain DHA levels and even contribute to the long-term benefits of maternal DHA supplementation during lactation on cognitive functions of toddlers and preschool children (Helland et al. 2003; Jensen et al. 2005). Together, our results underline that micronutrients, including dietary lipids, can support the wiring of neuronal networks and cortical information processing in the maturing brain.

Funding

Mead Johnson Nutrition (to T.B. and NeuroProof).

Notes

The funder had no role in the conceptualization, design, data collection, analysis, or preparation of the manuscript. No author has personal financial or non-financial competing interests. We are grateful to Dr Dirk Hondmann (Mead Johnson Nutrition) for discussions and acknowledge the project input by Chenzhong Kuang and Yan Xiao (Mead Johnson Nutrition Global Discovery). We thank Dr Michael C. Crair (Yale University School of Medicine) for enabling our in vivo recordings, Dr Ric van Tol (Mead Johnson Nutrition) for input and Dr Zhiping Pang and Joseph Fantuzzo (Rutgers University) for optimizing the Intellicount algorithm for immunohistochemistry. We thank the Tufts Center for Neuroscience Research for imaging support.

References

Aghajanian GK, Bloom FE. 1967. The formation of synaptic junctions in developing rat brain: a quantitative electron microscopic study. *Brain Res*. 6:716–727.

Anderson JW, Johnstone BM, Remley DT. 1999. Breast-feeding and cognitive development: a meta-analysis. *Am J Clin Nutr*. 70:525–535.

Bader BM, Steder A, Klein AB, Frolund B, Schroeder OHU, Jensen AA. 2017. Functional characterization of GABAA receptor-mediated modulation of cortical neuron network activity in microelectrode array recordings. *PLoS One*. 12:e0186147.

Barnett SA, Dickson RG. 1984. Milk production and consumption and growth of young of wild mice after ten generations in a cold environment. *J Physiol*. 346:409–417.

Bazinet RP, Laye S. 2014. Polyunsaturated fatty acids and their metabolites in brain function and disease. *Nat Rev Neurosci*. 15:771–785.

Benson DL, Huntley GW. 2012. Synapse adhesion: a dynamic equilibrium conferring stability and flexibility. *Curr Opin Neurobiol*. 22:397–404.

Bhatia HS, Agrawal R, Sharma S, Huo YX, Ying Z, Gomez-Pinilla F. 2011. Omega-3 fatty acid deficiency during brain maturation reduces neuronal and behavioral plasticity in adulthood. *PLoS One*. 6:e28451.

Biederer T, Scheiffele P. 2007. Mixed-culture assays for analyzing neuronal synapse formation. *Nat Protoc*. 2:670–676.

Birch D, Jacobs GH. 1979. Spatial contrast sensitivity in albino and pigmented rats. *Vision Res*. 19:933–937.

Birch EE, Carlson SE, Hoffman DR, Fitzgerald-Gustafson KM, Fu VL, Drover JR, Castaneda YS, Minns L, Wheaton DK, Mundy D *et al*. 2010. The DIAMOND (DHA Intake And Measurement Of Neural Development) Study: a double-masked, randomized controlled clinical trial of the maturation of infant visual acuity as a function of the dietary level of docosahexaenoic acid. *Am J Clin Nutr*. 91:848–859.

Downloaded from https://academic.oup.com/cercor/advance-article-abstract/doi/10.1093/cercor/bhz083/5480315 by Tufts University user on 29 April 2019

Bourre JM. 2004. Roles of unsaturated fatty acids (especially omega-3 fatty acids) in the brain at various ages and during ageing. *J Nutr Health Aging*. 8:163–174.

Bozek K, Wei Y, Yan Z, Liu X, Xiong J, Sugimoto M, Tomita M, Paabo S, Sherwood CC, Hof PR *et al*. 2015. Organization and evolution of brain lipidome revealed by large-scale analysis of human, chimpanzee, macaque, and mouse tissues. *Neuron*. 85:695–702.

Breckenridge WC, Gombos G, Morgan IG. 1972. The lipid composition of adult rat brain synaptosomal plasma membranes. *Biochim Biophys Acta*. 266:695–707.

Brenna JT, Varamini B, Jensen RG, Diersen-Schade DA, Boettcher JA, Arterburn LM. 2007. Docosahexaenoic and arachidonic acid concentrations in human breast milk worldwide. *Am J Clin Nutr*. 85:1457–1464.

Burgess A, Vigneron S, Brioudes E, Labbe JC, Lorca T, Castro A. 2010. Loss of human Greatwall results in G2 arrest and multiple mitotic defects due to deregulation of the cyclin B-Cdc2/PP2A balance. *Proc Natl Acad Sci USA*. 107:12564–12569.

Calder PC. 2012. Mechanisms of action of (n-3) fatty acids. *J Nutr*. 142:592S–599S.

Cancedda L, Putignano E, Sale A, Viegi A, Berardi N, Maffei L. 2004. Acceleration of visual system development by environmental enrichment. *J Neurosci*. 24:4840–4848.

Cao D, Kevala K, Kim J, Moon HS, Jun SB, Lovinger D, Kim HY. 2009. Docosahexaenoic acid promotes hippocampal neuronal development and synaptic function. *J Neurochem*. 111:510–521.

Cimafranca MA, Davila J, Ekman GC, Andrews RN, Neese SL, Peretz J, Woodling KA, Helferich WG, Sarkar J, Flaws JA *et al*. 2010. Acute and chronic effects of oral genistein administration in neonatal mice. *Biol Reprod*. 83:114–121.

Ciucci F, Putignano E, Baroncelli L, Landi S, Berardi N, Maffei L. 2007. Insulin-like growth factor 1 (IGF-1) mediates the effects of enriched environment (EE) on visual cortical development. *PLoS One*. 2:e475.

Connor S, Tenorio G, Clandinin MT, Sauve Y. 2012. DHA supplementation enhances high-frequency, stimulation-induced synaptic transmission in mouse hippocampus. *Appl Physiol Nutr Metab*. 37:880–887.

de Urquiza AM, Liu S, Sjoberg M, Zetterstrom RH, Griffiths W, Sjovall J, Perlmann T. 2000. Docosahexaenoic acid, a ligand for the retinoid X receptor in mouse brain. *Science*. 290:2140–2144.

Dobson V, Teller DY. 1978. Visual acuity in human infants: a review and comparison of behavioral and electrophysiological studies. *Vision Res*. 18:1469–1483.

Dombeck DA, Khabbaz AN, Collman F, Adelman TL, Tank DW. 2007. Imaging large-scale neural activity with cellular resolution in awake, mobile mice. *Neuron*. 56:43–57.

Dotti CG, Esteban JA, Ledesma MD. 2014. Lipid dynamics at dendritic spines. *Front Neuroanat*. 8:76.

Espinosa JS, Stryker MP. 2012. Development and plasticity of the primary visual cortex. *Neuron*. 75:230–249.

Fagiolini M, Pizzorusso T, Berardi N, Domenici L, Maffei L. 1994. Functional postnatal development of the rat primary visual cortex and the role of visual experience: dark rearing and monocular deprivation. *Vision Res*. 34:709–720.

Fantuzzo JA, Mirabella VR, Hamod AH, Hart RP, Zahn JD, Pang ZP. 2017. Intellicount: high-throughput quantification of fluorescent synaptic protein puncta by machine learning. *eNeuro*. 4: pii: ENEURO. 0219–0217.2017.

Feng X, Bader BM, Yang F, Segura M, Schultz L, Schroder OH, Rolfs A, Luo J. 2018. Improvement of impaired electrical activity in NPC1 mutant cortical neurons upon DHPG stimulation detected by micro-electrode array. *Brain Res*. 1694:87–93.

Ferreira TA, Blackman AV, Oyrer J, Jayabal S, Chung AJ, Watt AJ, Sjostrom PJ, van Meyel DJ. 2014. Neuronal morphometry directly from bitmap images. *Nat Methods*. 11:982–984.

Freeman DN, Marg E. 1975. Visual acuity development coincides with the sensitive period in kittens. *Nature*. 254:614–615.

Frenkel MY, Bear MF. 2004. How monocular deprivation shifts ocular dominance in visual cortex of young mice. *Neuron*. 44:917–923.

Gamoh S, Hashimoto M, Sugioka K, Shahdat Hossain M, Hata N, Misawa Y, Masumura S. 1999. Chronic administration of docosahexaenoic acid improves reference memory-related learning ability in young rats. *Neuroscience*. 93:237–241.

Goda Y, Davis GW. 2003. Mechanisms of synapse assembly and disassembly. *Neuron*. 40:243–264.

Gramowski-Voss A, Schwertle HJ, Pielka AM, Schultz L, Steder A, Jugelt K, Axmann J, Pries W. 2015. Enhancement of cortical network activity in vitro and promotion of GABAergic neurogenesis by stimulation with an electromagnetic field with a 150 MHz carrier wave pulsed with an alternating 10 and 16 Hz modulation. *Front Neurol*. 6:158.

Gramowski A, Jugelt K, Stuwe S, Schulze R, McGregor GP, Wartenberg-Demand A, Loock J, Schroder O, Weiss DG. 2006. Functional screening of traditional antidepressants with primary cortical neuronal networks grown on multielectrode neurochips. *Eur J Neurosci*. 24:455–465.

Harvey CD, Svoboda K. 2007. Locally dynamic synaptic learning rules in pyramidal neuron dendrites. *Nature*. 450:1195–1200.

Hashimoto M, Hossain S, Yamasaki H, Yazawa K, Masumura S. 1999. Effects of eicosapentaenoic acid and docosahexaenoic acid on plasma membrane fluidity of aortic endothelial cells. *Lipids*. 34:1297–1304.

Heimel JA, Hartman RJ, Hermans JM, Levelt CN. 2007. Screening mouse vision with intrinsic signal optical imaging. *Eur J Neurosci*. 25:795–804.

Helland IB, Smith L, Saarem K, Saugstad OD, Drevon CA. 2003. Maternal supplementation with very-long-chain n-3 fatty acids during pregnancy and lactation augments children's IQ at 4 years of age. *Pediatrics*. 111:e39–e44.

Högyes E, Nyakas C, Kiliaan A, Farkas T, Penke B, Luiten PG. 2003. Neuroprotective effect of developmental docosahexaenoic acid supplement against excitotoxic brain damage in infant rats. *Neuroscience*. 119:999–1012.

Holguin S, Huang Y, Liu J, Wurtman R. 2008. Chronic administration of DHA and UMP improves the impaired memory of environmentally impoverished rats. *Behav Brain Res*. 191:11–16.

Huang EJ, Reichardt LF. 2001. Neurotrophins: roles in neuronal development and function. *Annu Rev Neurosci*. 24:677–736.

Huang ZJ, Kirkwood A, Pizzorusso T, Porciatti V, Morales B, Bear MF, Maffei L, Tonegawa S. 1999. BDNF regulates the maturation of inhibition and the critical period of plasticity in mouse visual cortex. *Cell*. 98:739–755.

Huttenlocher PR, de Courten C, Garey LJ, Van der Loos H. 1982. Synaptogenesis in human visual cortex—evidence for synapse elimination during normal development. *Neurosci Lett*. 33:247–252.

Igarashi M, Santos RA, Cohen-Cory S. 2015. Impact of maternal n-3 polyunsaturated fatty acid deficiency on dendritic arbor morphology and connectivity of developing Xenopus laevis central neurons in vivo. *J Neurosci*. 35:6079–6092.

Innis SM. 2008. Dietary omega 3 fatty acids and the developing brain. *Brain Res*. 1237:35–43.

Downloaded from https://academic.oup.com/cercor/advance-article-abstract/doi/10.1093/cercor/bhz083/5480315 by Tufts University user on 29 April 2019

Ito D, Komatsu T, Gohara K. 2013. Measurement of saturation processes in glutamatergic and GABAergic synapse densities during long-term development of cultured rat cortical networks. *Brain Res*. 1534:22–32.

Jensen CL, Voigt RG, Prager TC, Zou YL, Fraley JK, Rozelle JC, Turcich MR, Llorente AM, Anderson RE, Heird WC. 2005. Effects of maternal docosahexaenoic acid intake on visual function and neurodevelopment in breastfed term infants. *Am J Clin Nutr*. 82:125–132.

Katz LC, Shatz CJ. 1996. Synaptic activity and the construction of cortical circuits. *Science*. 274:1133–1138.

Kim HY, Moon HS, Cao D, Lee J, Kevala K, Jun SB, Lovinger DM, Akbar M, Huang BX. 2011a. N-Docosahexaenoylethanolamide promotes development of hippocampal neurons. *Biochem J*. 435:327–336.

Kim HY, Spector AA, Xiong ZM. 2011b. A synaptogenic amide N-docosahexaenoylethanolamide promotes hippocampal development. *Prostaglandins Other Lipid Mediat*. 96:114–120.

Kitajka K, Puskas LG, Zvara A, Hackler L Jr, Barcelo-Coblijn G, Yeo YK, Farkas T. 2002. The role of n-3 polyunsaturated fatty acids in brain: modulation of rat brain gene expression by dietary n-3 fatty acids. *Proc Natl Acad Sci USA*. 99:2619–2624.

Kramer MS, Aboud F, Mironova E, Vanilovich I, Platt RW, Matush L, Igumnov S, Fombonne E, Bogdanovich N, Ducruet T *et al*. 2008. Breastfeeding and child cognitive development: new evidence from a large randomized trial. *Arch Gen Psychiatry*. 65:578–584.

Kuhlman SJ, Olivas ND, Tring E, Ikrar T, Xu X, Trachtenberg JT. 2013. A disinhibitory microcircuit initiates critical-period plasticity in the visual cortex. *Nature*. 501:543–546.

Lee JW, Huang BX, Kwon H, Rashid MA, Kharebava G, Desai A, Patnaik S, Marugan J, Kim HY. 2016. Orphan GPR110 (ADGRF1) targeted by N-docosahexaenoylethanolamine in development of neurons and cognitive function. *Nat Commun*. 7:13123.

Longair MH, Baker DA, Armstrong JD. 2011. Simple Neurite Tracer: open source software for reconstruction, visualization and analysis of neuronal processes. *Bioinformatics*. 27:2453–2454.

Lozada LE, Desai A, Kevala K, Lee JW, Kim HY. 2017. Perinatal brain docosahexaenoic acid concentration has a lasting impact on cognition in mice. *J Nutr*. 147:1624–1630.

Lucas A, Morley R, Cole TJ, Lister G, Leeson-Payne C. 1992. Breast milk and subsequent intelligence quotient in children born preterm. *Lancet*. 339:261–264.

Makrides M, Neumann MA, Byard RW, Simmer K, Gibson RA. 1994. Fatty acid composition of brain, retina, and erythrocytes in breast- and formula-fed infants. *Am J Clin Nutr*. 60:189–194.

Manni MM, Tiberti ML, Pagnotta S, Barelli H, Gautier R, Antonny B. 2018. Acyl chain asymmetry and polyunsaturation of brain phospholipids facilitate membrane vesiculation without leakage. *eLife*. 7:pii: e34394.

Mardinly AR, Spiegel I, Patrizi A, Centofante E, Bazinet JE, Tzeng CP, Mandel-Brehm C, Harmin DA, Adesnik H, Fagiolini M *et al*. 2016. Sensory experience regulates cortical inhibition by inducing IGF1 in VIP neurons. *Nature*. 531:371–375.

Marszalek JR, Lodish HF. 2005. Docosahexaenoic acid, fatty acid-interacting proteins, and neuronal function: breast-milk and fish are good for you. *Annu Rev Cell Dev Biol*. 21: 633–657.

Mayer DL, Dobson V. 1982. Visual acuity development in infants and young children, as assessed by operant preferential looking. *Vision Res*. 22:1141–1151.

McCann JC, Ames BN. 2005. Is docosahexaenoic acid, an n-3 long-chain polyunsaturated fatty acid, required for development of normal brain function? An overview of evidence from cognitive and behavioral tests in humans and animals. *Am J Clin Nutr*. 82:281–295.

McNamara RK, Carlson SE. 2006. Role of omega-3 fatty acids in brain development and function: potential implications for the pathogenesis and prevention of psychopathology. *Prostaglandins Leukot Essent Fatty Acids*. 75:329–349.

Meyer D, Bonhoeffer T, Scheuss V. 2014. Balance and stability of synaptic structures during synaptic plasticity. *Neuron*. 82:430–443.

Micheva KD, Beaulieu C. 1996. Quantitative aspects of synaptogenesis in the rat barrel field cortex with special reference to GABA circuitry. *J Comp Neurol*. 373:340–354.

Molloy C, Doyle LW, Makrides M, Anderson PJ. 2012. Docosahexaenoic acid and visual functioning in preterm infants: a review. *Neuropsychol Rev*. 22:425–437.

Moriguchi T, Greiner RS, Salem N Jr. 2000. Behavioral deficits associated with dietary induction of decreased brain docosahexaenoic acid concentration. *J Neurochem*. 75:2563–2573.

Muskiet FA, Fokkema MR, Schaafsma A, Boersma ER, Crawford MA. 2004. Is docosahexaenoic acid (DHA) essential? Lessons from DHA status regulation, our ancient diet, epidemiology and randomized controlled trials. *J Nutr*. 134:183–186.

Nguyen LN, Ma D, Shui G, Wong P, Cazenave-Gassiot A, Zhang X, Wenk MR, Goh EL, Silver DL. 2014. Mfsd2a is a transporter for the essential omega-3 fatty acid docosahexaenoic acid. *Nature*. 509:503–506.

Niell CM, Stryker MP. 2008. Highly selective receptive fields in mouse visual cortex. *J Neurosci*. 28:7520–7536.

Niell CM, Stryker MP. 2010. Modulation of visual responses by behavioral state in mouse visual cortex. *Neuron*. 65:472–479.

Odawara A, Katoh H, Matsuda N, Suzuki I. 2016. Physiological maturation and drug responses of human induced pluripotent stem cell-derived cortical neuronal networks in long-term culture. *Sci Rep*. 6:26181.

Oosting A, Verkade HJ, Kegler D, van de Heijning BJ, van der Beek EM. 2015. Rapid and selective manipulation of milk fatty acid composition in mice through the maternal diet during lactation. *J Nutr Sci*. 4:e19.

Park H, Poo MM. 2013. Neurotrophin regulation of neural circuit development and function. *Nat Rev Neurosci*. 14:7–23.

Paxinos G, Franklin KB. 2004. The mouse brain in stereotaxic coordinates. San Diego: Academic Press.

Pinot M, Vanni S, Pagnotta S, Lacas-Gervais S, Payet LA, Ferreira T, Gautier R, Goud B, Antonny B, Barelli H. 2014. Lipid cell biology. Polyunsaturated phospholipids facilitate membrane deformation and fission by endocytic proteins. *Science*. 345:693–697.

Porciatti V, Pizzorusso T, Maffei L. 1999. The visual physiology of the wild type mouse determined with pattern VEPs. *Vision Res*. 39:3071–3081.

Prusky GT, Douglas RM. 2003. Developmental plasticity of mouse visual acuity. *Eur J Neurosci*. 17:167–173.

Rakic P, Bourgeois JP, Eckenhoff MF, Zecevic N, Goldman-Rakic PS. 1986. Concurrent overproduction of synapses in diverse regions of the primate cerebral cortex. *Science*. 232:232–235.

Rath EA, Thenen SW. 1979. Use of tritiated water for measurement of 24-hour milk intake in suckling lean and genetically obese (ob/ob) mice. *J Nutr*. 109:840–847.

Downloaded from https://academic.oup.com/cercor/advance-article-abstract/doi/10.1093/cercor/bhz083/5480315 by Tufts University user on 29 April 2019

Rice DC, Reeve EA, Herlihy A, Zoeller RT, Thompson WD, Markowski VP. 2007. Developmental delays and locomotor activity in the C57BL6/J mouse following neonatal exposure to the fully-brominated PBDE, decabromodiphenyl ether. *Neurotoxicol Teratol*. 29:511–520.

Ridder WH 3rd, Nusinowitz S. 2006. The visual evoked potential in the mouse—origins and response characteristics. *Vision Res*. 46:902–913.

Sakamoto T, Cansev M, Wurtman RJ. 2007. Oral supplementation with docosahexaenoic acid and uridine-5′-monophosphate increases dendritic spine density in adult gerbil hippocampus. *Brain Res*. 1182:50–59.

Sale A, Putignano E, Cancedda L, Landi S, Cirulli F, Berardi N, Maffei L. 2004. Enriched environment and acceleration of visual system development. *Neuropharmacology*. 47:649–660.

Salem N Jr, Litman B, Kim HY, Gawrisch K. 2001. Mechanisms of action of docosahexaenoic acid in the nervous system. *Lipids*. 36:945–959.

SanGiovanni JP, Parra-Cabrera S, Colditz GA, Berkey CS, Dwyer JT. 2000. Meta-analysis of dietary essential fatty acids and long-chain polyunsaturated fatty acids as they relate to visual resolution acuity in healthy preterm infants. *Pediatrics*. 105:1292–1298.

Schreiner D, Savas JN, Herzog E, Brose N, de Wit J. 2017. Synapse biology in the 'circuit-age'-paths toward molecular connectomics. *Curr Opin Neurobiol*. 42:102–110.

Shen K, Scheiffele P. 2010. Genetics and cell biology of building specific synaptic connectivity. *Annu Rev Neurosci*. 33:473–507.

Sholl DA. 1953. Dendritic organization in the neurons of the visual and motor cortices of the cat. *J Anat*. 87:387–406.

Sidhu VK, Huang BX, Kim HY. 2011. Effects of docosahexaenoic acid on mouse brain synaptic plasma membrane proteome analyzed by mass spectrometry and (16)O/(18)O labeling. *J Proteome Res*. 10:5472–5480.

Smit EN, Martini IA, Mulder H, Boersma ER, Muskiet FA. 2002. Estimated biological variation of the mature human milk fatty acid composition. *Prostaglandins Leukot Essent Fatty Acids*. 66:549–555.

Stillwell W, Shaikh SR, Zerouga M, Siddiqui R, Wassall SR. 2005. Docosahexaenoic acid affects cell signaling by altering lipid rafts. *Reprod Nutr Dev*. 45:559–579.

Tulodziecka K, Diaz-Rohrer BB, Farley MM, Chan RB, Di Paolo G, Levental KR, Waxham MN, Levental I. 2016. Remodeling of the postsynaptic plasma membrane during neural development. *Mol Biol Cell*. 27:3480–3489.

Uauy R, Hoffman DR, Peirano P, Birch DG, Birch EE. 2001. Essential fatty acids in visual and brain development. *Lipids*. 36:885–895.

Workman AD, Charvet CJ, Clancy B, Darlington RB, Finlay BL. 2013. Modeling transformations of neurodevelopmental sequences across mammalian species. *J Neurosci*. 33: 7368–7383.

Wu A, Ying Z, Gomez-Pinilla F. 2004. Dietary omega-3 fatty acids normalize BDNF levels, reduce oxidative damage, and counteract learning disability after traumatic brain injury in rats. *J Neurotrauma*. 21:1457–1467.

Wu A, Ying Z, Gomez-Pinilla F. 2008. Docosahexaenoic acid dietary supplementation enhances the effects of exercise on synaptic plasticity and cognition. *Neuroscience*. 155:751–759.

Zweifel LS, Kuruvilla R, Ginty DD. 2005. Functions and mechanisms of retrograde neurotrophin signalling. *Nat Rev Neurosci*. 6:615–625.

Downloaded from https://academic.oup.com/cercor/advance-article-abstract/doi/10.1093/cercor/bhz083/5480315 by Tufts University user on 29 April 2019